



Yüksek Hassasiyetli Uygulamalar için DC-DC Buck Dönüştürücünün Otomatik Ayarlamalı PID Kontrolü

Adile AKPUNAR BOZKURT ^{1*} 

¹Mekatronik Mühendisliği, Teknoloji Fakültesi, Pamukkale Üniversitesi, Denizli, Türkiye.

¹aakpunar@pau.edu.tr

Geliş Tarihi: 13.1.2025
Kabul Tarihi: 02.11.2025

Düzeltilme Tarihi: 27.5.2025

doi: <https://doi.org/10.62520/fujece.1619005>
Araştırma Makalesi

Alıntı: A. A. Bozkurt, “Yüksek hassasiyetli uygulamalar için DC-DC buck dönüştürücünün otomatik ayarlamalı PID kontrolü” Fırat Üni. Deny. ve Hes. Müh. Derg., vol. 5, no 1, pp. 135-149, Şubat 2026.

Öz

DC-DC dönüştürücüler, motor sürücü sistemleri, yenilenebilir enerji kaynakları ve bilgisayar güç kaynakları gibi çok çeşitli uygulamalarda temel bileşenlerdir. Bu dönüştürücüler, değişken yük koşulları altında, regüle edilmemiş bir giriş geriliminden kararlı bir doğru akım (DC) çıkışı elde etmek amacıyla kullanılır. İstenen çıkış gerilimi seviyesine bağlı olarak çeşitli dönüştürücü topolojileri geliştirilmiştir. Bunlar arasında buck (alçaltıcı) dönüştürücü, giriş gerilimini verimli bir şekilde düşürebilme özelliği sayesinde en yaygın şekilde benimsenen çözümlerden biridir. Çıkış geriliminin belirlenmiş bir referans değere yakın tutulabilmesi için genellikle kapalı çevrimli çeşitli kontrol stratejileri uygulanmaktadır. Bu çalışma, DC-DC buck dönüştürücüsünün çıkış gerilimini hassas bir şekilde regüle etmek amacıyla, modele dayalı otomatik ayarlamalı bir Oransal-İntegral-Türevsel (PID) kontrol algoritmasının uygulanmasını sunmaktadır. Sabit kazanç parametreleriyle çalışan klasik PID denetleyiciler, sistem parametrelerindeki değişimlere ve dış bozululara karşı sınırlı bir uyum kabiliyeti sergilerken; önerilen kontrolör, parametrelerini gerçek zamanlı olarak dinamik şekilde ayarlayarak değişen çalışma koşullarına daha iyi uyum sağlamaktadır. Bu uyarlanabilir yapı, sistemin değişken işletim koşulları altında dayanıklılığını artırmaktadır. Simülasyon sonuçları, önerilen yöntemin etkinliğini doğrulamakta; hızlı geçici tepki, minimum aşım ve yüksek kararlı durum kararlılığı sağladığını ortaya koymaktadır. Elde edilen bulgular, özellikle ayarlamalı ve yüksek hassasiyetli regülasyon gerektiren gömülü sistem uygulamaları için önerilen yaklaşımın pratik ve etkili bir kontrol çözümü sunduğunu göstermektedir.

Anahtar kelimeler: DC-DC Buck dönüştürücü, PID denetleyici, Doğrusal olmayan kontrol, Gerilim regülasyonu

*Yazışılan yazar

İntihal Kontrol: Evet – Turnitin

Şikayet: fujece@firat.edu.tr

Telif Hakkı ve Lisans: Dergide yayın yapan yazarlar, CC BY-NC 4.0 kapsamında lisanslanan çalışmalarının telif hakkını saklı tutar



Auto-Tuning PID Control of a DC-DC Buck Converter for High-Precision Applications

Adile AKPUNAR BOZKURT^{1*}  

¹ Department of Mechatronics Engineering, Faculty of Technology, Pamukkale University, Denizli, Türkiye.
¹aakpunar@pau.edu.tr

Received: 13.1.2025
Accepted: 02.11.2025

Revision: 27.5.2025

doi: <https://doi.org/10.62520/fujece.1619005>
Research Article

Citation: A. A. Bozkurt, "Auto-tuning PID control of a DC-DC buck converter for high-precision applications" *Firat Univ Jour. of Exp. and Comp. Eng.*, vol. 5, no 1, pp. 135-149, February 2026.

Abstract

DC-DC converters are essential components in a wide range of applications, including motor drive systems, renewable energy sources, and computer power supplies. These converters regulate an unregulated input voltage to provide a stable DC output under varying load conditions. Depending on the desired voltage level, several converter topologies have been developed. Among them, the buck converter stands out as one of the most widely adopted solutions due to its ability to step down the input voltage efficiently. To ensure that the output voltage remains close to a predefined reference value, various closed-loop control strategies are commonly employed. This study presents the implementation of a model-based, auto-tuning Proportional–Integral–Derivative (PID) control algorithm for precise output voltage regulation in a DC-DC buck converter. Unlike classical PID controllers, which operate with fixed gain parameters and exhibit limited adaptability to parameter variations and external disturbances, the proposed controller dynamically adjusts its parameters in real time. This adaptive capability enhances the system's robustness under varying operating conditions. Simulation results validate the effectiveness of the proposed method, demonstrating fast transient response, minimal overshoot, and high steady-state stability. These findings suggest that the approach offers a practical and efficient control solution, especially for embedded systems requiring adaptive and high-precision regulation.

Keywords: DC-DC Buck converter, PID controller, Nonlinear control, Voltage regulation

*Corresponding author

1. Introduction

In recent years, power circuits have found a wide range of applications and gained great popularity [1]. Among these circuits, DC-DC converters stand out as one of the basic components in the power circuit family [2]. DC-DC converters, fundamental circuits in power electronics, operate by switching to modify electrical voltage levels and are increasingly utilized across various applications [3]. They provide an adjustable DC voltage from an unregulated source to a variable load.

By leveraging semiconductor switching elements, DC-DC converters serve as compact, lightweight, and highly efficient solutions for DC power conversion. Under normal operating conditions, they can respond quickly and appropriately to changes in input voltage and return to normal operation [4]. These converters are widely used in various applications such as televisions, battery chargers, receivers, computers, medical devices, communication equipment, and military hardware [5]. In industrial applications, buck converters are commonly employed to achieve the conversion of high DC input voltages into reduced DC output levels [6].

In [3], the use of DC/DC converters in mobile devices is examined, with a focus on the operation of the buck converter using a PID controller. In [7], a new multi-level DC-DC buck converter topology with clamped diodes for DC motors has been presented. In [8], Buck-type DC-DC converters are introduced as a solution for regulating both the charging voltage and current in battery charging systems for electric vehicles. In [9], a DC-DC buck converter has been used in the charge controllers of wind energy systems. In [10], a detailed performance evaluation of a synchronous buck converter implemented for a photovoltaic (PV) system was presented.

In terms of control of DC-DC converters, these systems, being switched power converters, present a challenging field of study due to their variable and nonlinear structure. Rapid structural changes are usually handled using averaging models. In [11, 12], a PWM-based sliding mode voltage-controlled (SMVC) buck converter design has been presented. In [13], a model predictive control (MPC) design was proposed for controlling a fixed-frequency DC-DC power converter.

An auto-tuning method based on the Modified Relay Feedback Test (MRFT) has been designed and implemented for PID voltage-mode control of DC-DC buck converters [14]. Similarly, a fuzzy extended model reference adaptive voltage regulation strategy was proposed to enhance robustness against random input fluctuations and load transients in DC-DC buck converters [15]. Another study examined the effectiveness of the Archimedes Optimization Algorithm (AOA) as a metaheuristic approach for tuning PID controllers in closed-loop DC-DC buck converters, achieving stable output voltage regulation [16]. Moreover, the design and implementation of a digital PID controller, specifically tailored for DC-DC buck converters, was carried out using MATLAB as the primary simulation and development platform [17].

DC-DC buck converters are widely used in various industrial and portable electronic systems that require either constant or variable voltage levels. To maintain stable output voltage regulation in such converters, PID controllers are commonly employed. However, variations in system parameters and the dynamic nature of load conditions often limit the effectiveness of fixed-gain PID controllers. In response to these limitations, PID control strategies incorporating auto-tuning mechanisms have gained increasing attention in recent years. In this study, a model-based auto-tuning PID control approach is proposed and implemented for a DC-DC buck converter to achieve both faster and more stable voltage regulation, while simultaneously enabling the system to adapt to time-varying dynamics. Unlike conventional fixed-parameter methods, the proposed structure continuously adjusts the controller gains in real-time, thereby optimizing system performance under changing conditions.

The control strategy is based on an auto-tuning PID method that is well-suited for the robust regulation of nonlinear systems, as discussed in [18, 19]. The entire control system is implemented in the MATLAB/Simulink environment. Simulation results demonstrate that the proposed controller regulates the output voltage more rapidly and effectively compared to conventional PID methods. Furthermore, key performance indicators such as transient response, overshoot, and stability are quantitatively evaluated to

highlight the advantages of the auto-tuning approach. The following sections provide a detailed presentation of the DC-DC buck converter model, the conventional PID control structure, the proposed auto-tuning PID strategy, and simulation-based performance comparisons.

2. Material and Method

2.1. Model of the DC-DC buck converter

The DC-DC buck converter circuit's design and analysis assume that the inductor current operates in continuous current mode (CCM), the output voltage is kept constant, and the circuit operates in a steady state [20]. Figure 1 shows the buck converter circuit.

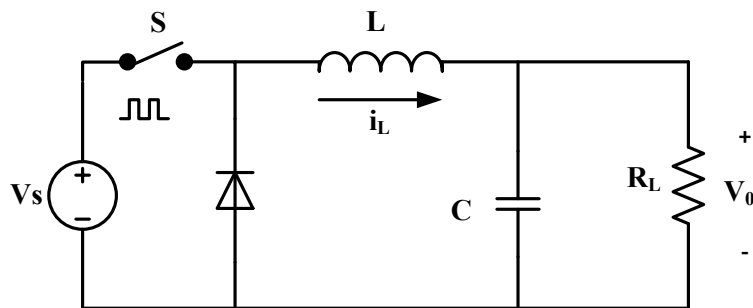


Figure 1. DC-DC Buck Converter circuit [20]

This circuit operates in two modes: the mode in which the switch is open and the mode in which the switch is closed. According to these operating modes, the mathematical equations of the buck converter are obtained. MOSFET, IGBT, or BJT can be used as the switch. The dynamic behavior of the DC-DC buck converter is defined according to each switching mode. Figure 2 shows the switch-off and switch-on states of the buck converter.

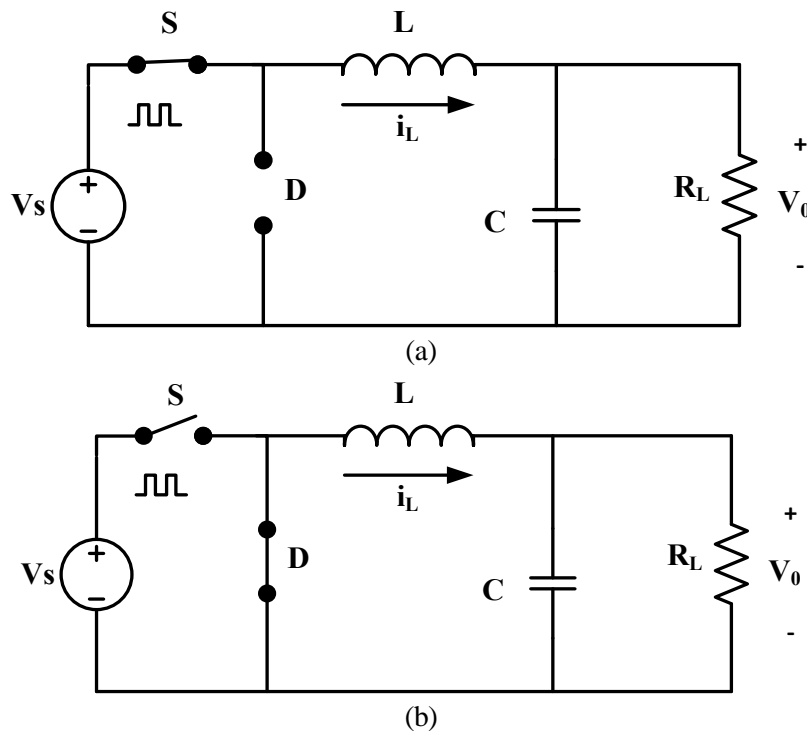


Figure 2. Switch states. (a) closed, (b) opened

As illustrated in Figure 2a, when the switch is in the closed position, the DC source supplies current to the inductor and load resistor, causing the diode to be reverse-biased. Thus, the dynamic equation can be expressed as:

$$V_s = L \frac{di_L}{dt} + V_c \quad (1)$$

$$i_L = C \frac{dV_c}{dt} + \frac{V_c}{R} \quad (2)$$

As shown in Figure 2b, opening the switch causes the diode to become forward-biased, directing the inductor current through the load resistor. Thus, the dynamic equation ([2], [21]) is expressed as:

$$0 = L \frac{di_L}{dt} + V_c \quad (3)$$

If the control signal u is defined as

$$u = \begin{cases} 1, & 0 \leq t < t_{on} \\ 0, & t_{on} \leq t \leq T \end{cases}$$

The general equation describing the DC-DC buck converter can be written as

$$\frac{di_L}{dt} = -\frac{1}{L}V_c + \frac{V_s}{L}u \quad (4)$$

$$\frac{dV_c}{dt} = \frac{1}{C}i_L - \frac{1}{RC}V_c \quad (5)$$

In this context, i_L refers to the inductor current, while V_c corresponds to the capacitor voltage ([2], [21]). These are the state variables defining the Buck converter. The specifications of the DC-DC buck converter are listed in Table 1.

Table 1. Specifications of the DC-DC buck converter

Parameters	Symbol	Value
Input Voltage	V_s	20V
Output Voltage	V_o	12V
Load	R_L	2.5 Ω
Inductance	L	4mH
Capacitance	C	47uF

In DC-DC buck converters, the values of inductance and capacitance are selected based on the desired current ripple (ΔI_L) and voltage ripple (ΔV). In this study, ΔI_L is set to 48mA and ΔV to 5mV. These ripple levels are suitable for high-precision power applications.

The inductance required to ensure Continuous Conduction Mode (CCM) operation of the buck converter can be calculated using Equation 6, while the required capacitance value can be determined from Equation 7.

$$L = \frac{(V_{in} - V_{out}) \cdot D}{\Delta I_L \cdot F_s} \approx 4mH \quad (6)$$

$$C = \frac{(V_{in} - V_{out}) \cdot D}{8F_s^2 L \Delta V} \approx 47\mu F \quad (7)$$

Here, V_{in} is the input voltage, V_{out} is the output voltage, D is the duty cycle, and F_s is the switching frequency [22].

2.2. PID controller

PID controllers are among the most commonly used feedback control strategies, particularly for linear systems. The general structure of a classical PID controller is illustrated in Figure 3.

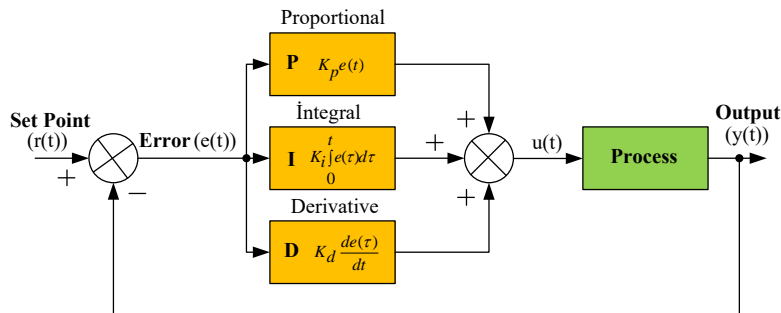


Figure 3. General structure of a PID controller [24]

The PID controller generates an error signal based on the difference between the reference signal $r(t)$ and the output signal $y(t)$, as given in Equation (8):

$$e(t) = r(t) - y(t) \quad (8)$$

The main objective of the controller is to minimize this error signal, thereby ensuring the system exhibits the desired behavior. The PID controller consists of a combination of proportional (P), integral (I), and derivative (D) terms. These three components form the control law expressed in Equation (9):

$$u(t) = K_p e(t) + K_i \int_0^t e(\tau) d\tau + K_d \frac{de(t)}{dt} \quad (9)$$

The proportional gain K_p provides an immediate response proportional to the error signal. However, when used alone, it cannot completely eliminate the steady-state error. The integral gain K_i eliminates steady-state error over time by accumulating the error, enabling the system to reach the reference value. Nonetheless, excessive integral gain may lead to overshoot and instability. The derivative gain K_d improves the transient response by predicting future error behavior, helping reduce overshoot and stabilize the system.

Proper tuning of PID parameters is critical for achieving desired system performance. Empirical methods such as Ziegler–Nichols and Cohen–Coon are frequently used for this purpose. The effects of PID gain variations on system response are summarized in Table 2 [23, 24].

Table 2. Effects of PID gains on system response

<i>PID gain</i>	<i>Steady state error</i>	<i>Setting time</i>	<i>Percent Overshoot</i>
<i>Increasing K_p</i>	Decreases	Slightly increasing	Increases
<i>Increasing K_i</i>	Eliminate	Increases	Increases
<i>Increasing K_d</i>	Slight Change	Decreases	Decreases

2.3. Auto-tuning PID

The DC-DC Buck converter plays a crucial role in maintaining efficient voltage regulation under varying operating conditions. An auto-tuning PID controller is implemented to achieve precise control, dynamically generating the control input signal, denoted as u . This signal works to minimize the difference between the measured output voltage of the converter and the target reference voltage.

The structural configuration of the DC-DC Buck converter and the auto-tuning PID controller is illustrated in Figure 4. The controller continuously adjusts the system parameters to maintain optimal performance. The converter's switching frequency is set to 25 kHz, corresponding to a sampling period of 40 μ s, ensuring real-time adaptability of the control mechanism.

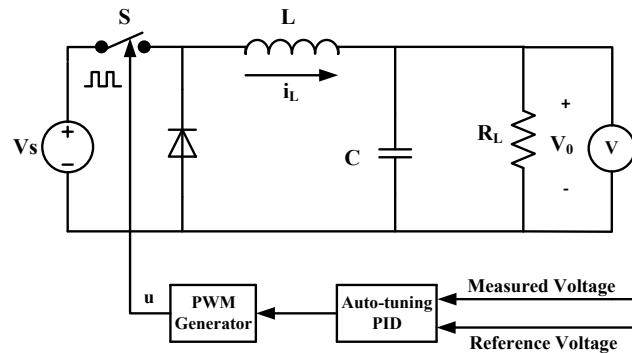


Figure 4. Configuration of the DC-DC buck converter and controller

The configuration of the proposed auto-tuning PID controller is shown in Figure 5. This model-based PID controller incorporates a discrete system model, two Jacobian blocks, and an adaptive PID block, each serving distinct purposes to ensure optimal performance. One Jacobian block refines the control signal, while the other facilitates parameter tuning. The adaptive PID block dynamically adjusts controller parameters to minimize the error signal.

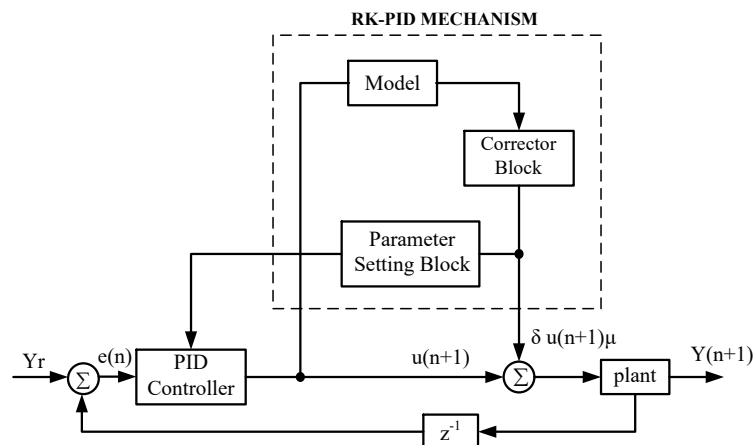


Figure 5. Auto-tuning PID controller structure ([18], [19])

In this configuration, Y_r represents the reference signal, $Y(n+1)$ denotes the system output at the next time step, $u(n+1)$ is the input control signal, and δu is the correction term applied to improve the control signal. The error e is computed as the difference between the reference and measured output signals.

In the system model of the PID control mechanism, two Jacobian matrices are utilized to enhance system performance. The matrix J_m serves to verify and refine the control signal, while J_c dynamically adjusts the PID control parameters to ensure optimal system response. Within this framework, the reference signal and the candidate input voltage are applied as inputs to the model.

As outputs, the system generates a K-fold prediction of the output signal and a verification term, which collectively guide the adjustment process. In the PID block, the proportional (K_P), integral (K_I), and derivative (K_D) parameters are computed and updated in real-time to adapt to changing system dynamics. Finally, the PID controller generates the control signal as defined in Equation 10 ([18], [19]).

$$\mathbf{u}(n + 1) = \mathbf{u}(n) + \mathbf{K}_p(\mathbf{e}(n) - \mathbf{e}(n - 1)) + \mathbf{K}_I\mathbf{e}(n) + \mathbf{K}_D(\mathbf{e}(n) - 2\mathbf{e}(n - 1) + \mathbf{e}(n - 2)) \quad (10)$$

The generated input signal $\mathbf{u}(n + 1)$ is fed to the system model K times. The PID parameters are determined by the objective function that minimizes the sum of squares of the prediction errors after K steps.

$$F(\mathbf{u}(n + 1)) = \frac{1}{2} \sum_{k=1}^K \sum_{j=1}^Q (\tilde{y}_j(n + k) - \hat{y}_j(n + k))^2 + \frac{1}{2} \lambda \sum_{r=1}^R (u_r(n + 1) - u_r(n))^2 \quad (11)$$

In this equation, k represents the estimation horizon, and λ represents the penalty parameter.

The Levenberg-Marquardt method is employed to minimize the objective function and concurrently update the PID parameters.

$$\begin{bmatrix} \mathbf{K}_p^{new} \\ \mathbf{K}_I^{new} \\ \mathbf{K}_D^{new} \end{bmatrix} = \begin{bmatrix} \mathbf{K}_p^{old} \\ \mathbf{K}_I^{old} \\ \mathbf{K}_D^{old} \end{bmatrix} - (\mathbf{J}^T\mathbf{J} + \mu\mathbf{I})^{-1}\mathbf{J}^T\hat{\mathbf{e}} \quad (12)$$

In this context, μ serves as a compromise between the Steepest-Descent and Gauss-Newton algorithms, while \mathbf{I} represents the identity matrix. The Jacobian matrix is defined in Equations 13 and 14 ([18], [19]).

$$\mathbf{J} = \begin{bmatrix} \frac{\partial \hat{e}_1(n + 1)}{\partial \mathbf{K}_p} & \frac{\partial \hat{e}_1(n + 1)}{\partial \mathbf{K}_I} & \frac{\partial \hat{e}_1(n + 1)}{\partial \mathbf{K}_D} \\ \vdots & \vdots & \vdots \\ \frac{\partial \hat{e}_Q(n + K)}{\partial \mathbf{K}_p} & \frac{\partial \hat{e}_Q(n + K)}{\partial \mathbf{K}_I} & \frac{\partial \hat{e}_Q(n + K)}{\partial \mathbf{K}_D} \\ \frac{\partial \sqrt{\lambda_1} \Delta \mathbf{u}(n + 1)}{\partial \mathbf{K}_p} & \frac{\partial \sqrt{\lambda_1} \Delta \mathbf{u}(n + 1)}{\partial \mathbf{K}_I} & \frac{\partial \sqrt{\lambda_1} \Delta \mathbf{u}(n + 1)}{\partial \mathbf{K}_D} \\ \vdots & \vdots & \vdots \\ \frac{\partial \sqrt{\lambda_R} \Delta \mathbf{u}(n + 1)}{\partial \mathbf{K}_p} & \frac{\partial \sqrt{\lambda_R} \Delta \mathbf{u}(n + 1)}{\partial \mathbf{K}_I} & \frac{\partial \sqrt{\lambda_R} \Delta \mathbf{u}(n + 1)}{\partial \mathbf{K}_D} \end{bmatrix} \quad (13)$$

$$\mathbf{J} = - \begin{bmatrix} \frac{\partial \hat{y}_1(n + 1)}{\partial \mathbf{K}_p} & \frac{\partial \hat{y}_1(n + 1)}{\partial \mathbf{K}_I} & \frac{\partial \hat{y}_1(n + 1)}{\partial \mathbf{K}_D} \\ \vdots & \vdots & \vdots \\ \frac{\partial \hat{y}_Q(n + K)}{\partial \mathbf{K}_p} & \frac{\partial \hat{y}_Q(n + K)}{\partial \mathbf{K}_I} & \frac{\partial \hat{y}_Q(n + K)}{\partial \mathbf{K}_D} \\ \frac{\partial \sqrt{\lambda_1} \Delta \mathbf{u}(n + 1)}{\partial \mathbf{K}_p} & \frac{\partial \sqrt{\lambda_1} \Delta \mathbf{u}(n + 1)}{\partial \mathbf{K}_I} & \frac{\partial \sqrt{\lambda_1} \Delta \mathbf{u}(n + 1)}{\partial \mathbf{K}_D} \\ \vdots & \vdots & \vdots \\ \frac{\partial \sqrt{\lambda_R} \Delta \mathbf{u}(n + 1)}{\partial \mathbf{K}_p} & \frac{\partial \sqrt{\lambda_R} \Delta \mathbf{u}(n + 1)}{\partial \mathbf{K}_I} & \frac{\partial \sqrt{\lambda_R} \Delta \mathbf{u}(n + 1)}{\partial \mathbf{K}_D} \end{bmatrix} \quad (14)$$

In Equation 15, the vector of forecast errors $\hat{\mathbf{e}}$ is given.

$$\hat{\mathbf{e}} = \begin{bmatrix} \hat{e}_1(n + 1) \\ \vdots \\ \hat{e}_Q(n + K) \\ \sqrt{\lambda_1} \Delta \mathbf{u}(n + 1) \\ \vdots \\ \sqrt{\lambda_R} \Delta \mathbf{u}(n + 1) \end{bmatrix} = \begin{bmatrix} \hat{y}_1(n + 1) - \hat{y}_1(n + 1) \\ \vdots \\ \hat{y}_1(n + K) - \hat{y}_1(n + K) \\ \sqrt{\lambda_1} \Delta \mathbf{u}(n + 1) \\ \vdots \\ \sqrt{\lambda_R} \Delta \mathbf{u}(n + 1) \end{bmatrix} \quad (15)$$

Here, $\Delta \mathbf{u}(n + 1)$ is defined as

$$\Delta \mathbf{u}(n + 1) = \mathbf{u}(n + 1) - \mathbf{u}(n) \quad (16)$$

At this stage, the PID parameters are updated step by step. The correction block is designed to minimize the objective function by applying the quadratic Taylor approximation ([18, 19]).

$$\begin{aligned}
 & F(\mathbf{u}(n+1) + \delta\mathbf{u}(n+1)) \\
 & \cong F(\mathbf{u}(n+1)) + \frac{\partial F(\mathbf{u}(n+1))}{\partial \mathbf{u}(n+1)} \delta\mathbf{u}(n+1) \\
 & + \frac{1}{2} \frac{\partial^2 F(\mathbf{u}(n+1))}{\partial \mathbf{u}^2(n+1)} (\delta\mathbf{u}(n+1))^2
 \end{aligned} \tag{17}$$

If the derivative of the objective function with respect to the $\delta\mathbf{u}(n+1)$ term is taken and set equal to zero,

$$\delta\mathbf{u}(n+1) = - \frac{\frac{\partial F}{\partial \mathbf{u}(n+1)}}{\frac{\partial^2 F}{\partial \mathbf{u}^2(n+1)}} \tag{18}$$

is obtained. Here, Jacobian approximations can be used instead of derivatives in Equation 18, as shown in the Jacobian formulation given by Equation 19 ([18, 19]).

$$\mathbf{J}_m = - \begin{bmatrix} \frac{\partial \hat{y}_1(n+1)}{\partial u_1(n+1)} & \frac{\partial \hat{y}_1(n+1)}{\partial u_2(n+1)} & \cdots & \frac{\partial \hat{y}_1(n+1)}{\partial u_R(n+1)} \\ \vdots & \vdots & \vdots & \vdots \\ \frac{\partial \hat{y}_Q(n+1)}{\partial u_1(n+1)} & \frac{\partial \hat{y}_Q(n+1)}{\partial u_2(n+1)} & \cdots & \frac{\partial \hat{y}_Q(n+1)}{\partial u_R(n+1)} \\ \sqrt{\lambda_1} & \sqrt{\lambda_1} & \cdots & \sqrt{\lambda_1} \\ \vdots & \vdots & \vdots & \vdots \\ \sqrt{\lambda_R} & \sqrt{\lambda_R} & \cdots & \sqrt{\lambda_R} \end{bmatrix} \tag{19}$$

Verification term is calculated from the Equation 20.

$$\delta\mathbf{u}(n+1) = - \frac{\mathbf{J}_m^T \hat{\mathbf{e}}}{\mathbf{J}_m^T \mathbf{J}_m} \tag{20}$$

The Jacobian matrix in Equation 14 can be written as $\mathbf{J} = \mathbf{J}_m \cdot \mathbf{J}_c$.

$$\mathbf{J} = - \begin{bmatrix} \frac{\partial \hat{y}_1(n+1)}{\partial u_1(n+1)} & \frac{\partial \hat{y}_1(n+1)}{\partial u_2(n+1)} & \cdots & \frac{\partial \hat{y}_1(n+1)}{\partial u_R(n+1)} \\ \vdots & \vdots & \vdots & \vdots \\ \frac{\partial \hat{y}_Q(n+1)}{\partial u_1(n+1)} & \frac{\partial \hat{y}_Q(n+1)}{\partial u_2(n+1)} & \cdots & \frac{\partial \hat{y}_Q(n+1)}{\partial u_R(n+1)} \\ \sqrt{\lambda_1} & \sqrt{\lambda_1} & \cdots & \sqrt{\lambda_1} \\ \vdots & \vdots & \vdots & \vdots \\ \sqrt{\lambda_R} & \sqrt{\lambda_R} & \cdots & \sqrt{\lambda_R} \end{bmatrix} \begin{bmatrix} \frac{\partial u_1(n+1)}{\partial K_{P11}} & \cdots & \frac{\partial u_1(n+1)}{\partial K_{D_{RQ}}} \\ \vdots & \vdots & \vdots \\ \frac{\partial u_R(n+1)}{\partial K_{P11}} & \cdots & \frac{\partial u_R(n+1)}{\partial K_{D_{RQ}}} \end{bmatrix} \tag{21}$$

\mathbf{K}_P , \mathbf{K}_I , and \mathbf{K}_D parameter values are adjusted in the PID block at each iteration ([18], [19]).

To implement the proposed control strategy, the auto-tuning PID algorithm is designed as shown below.

Input: Measured system outputs $\mathbf{y}(n)$, reference signal $\mathbf{y}_r(n)$, previous control input $\mathbf{u}(n)$

Output: Updated control input $\mathbf{u}(n+1)$, and updated PID parameters (\mathbf{K}_P , \mathbf{K}_I , \mathbf{K}_D)

1. Measure the system output $\mathbf{y}(n)$
2. Compute the tracking error: $\mathbf{e}(n) = \mathbf{y}_r(n) - \mathbf{y}(n)$
3. Calculate the initial control input: $\mathbf{u}(n+1)$
4. Predict future outputs: $[\hat{y}_1(n+1), \dots, \hat{y}_Q(n+K)]$
5. Compute the Jacobian matrices:
 - \mathbf{J}_m for verifying the control signal
 - \mathbf{J}_c for tuning the PID control parameters
6. Compute the control correction term: $\delta\mathbf{u}(n+1)$
7. Update PID parameters (\mathbf{K}_P , \mathbf{K}_I , \mathbf{K}_D) based on adaptation criteria
8. Update the control input signal: $\mathbf{u}(n+1) = \mathbf{u}(n) + \delta\mathbf{u}(n+1)$

9. Apply $u(n + 1)$ to the system

3. Simulation Results and Discussion

The study was conducted using the MATLAB/Simulink environment, where both the auto-tuning PID controller and the conventional PID controller were implemented and compared. In Figure 6, the output voltage of the DC-DC buck converter is depicted, with the system configured to operate at a constant reference voltage of 12 V. The auto-tuning PID controller reaches the desired output voltage in under 0.004 s, whereas the conventional PID controller takes 0.08 s to achieve the desired output voltage. No overshoot is observed in either controller during the transient phase.

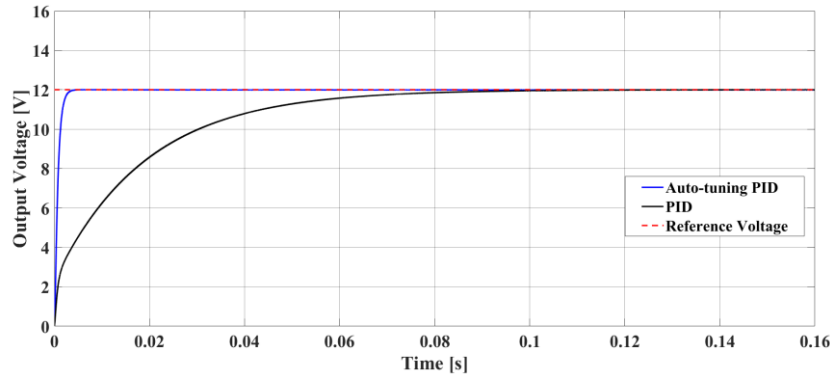


Figure 6. Output voltage waveform

Table 3 presents a comparative analysis of the transient response of the output voltage of the DC-DC buck converter.

Table 3. Comparison of the transient response of the DC-DC buck converter output voltage.

<i>Methods</i>	<i>Auto-tuning PID</i>	<i>PID</i>
<i>Setting time (s)</i>	0.004	0.08
<i>Rise time (s)</i>	0.002	0.06
<i>Overshoot (V)</i>	0	0
<i>Steady state voltage ripple (V)</i>	0.05	0.06

Figure 7 illustrates the output voltage profiles of the DC–DC buck converter under varying operating points. In this experiment, a step reference voltage was applied to evaluate the performance of the control mechanisms. Initially, the converter operated at 12 V, after which the reference voltage was decreased to 10 V at $t = 0.2$ s. Subsequently, at $t = 0.4$ s, the reference was restored to 12 V, and the converter continued its operation accordingly. Both the auto-tuning PID controller and the conventional PID controller successfully regulated the output voltage to track the desired reference without observable overshoot.

However, the auto-tuning PID controller demonstrated superior dynamic performance, achieving the desired reference voltage with a significantly shorter settling time compared to the conventional PID controller. This highlights the adaptive controller’s ability to respond more efficiently to changes in operating conditions.

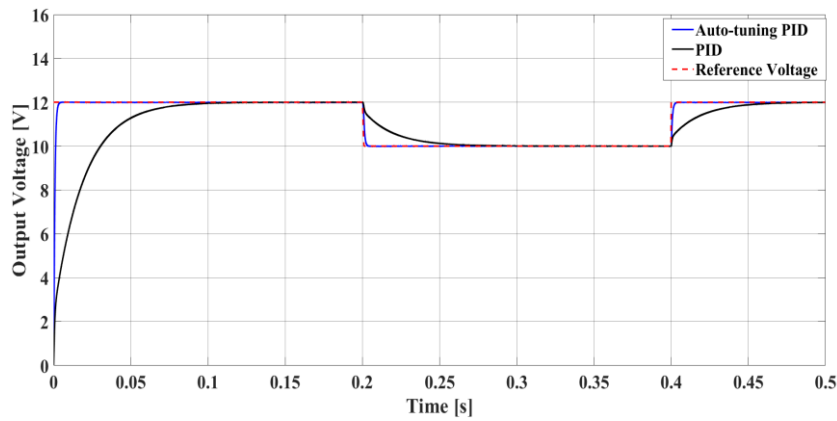


Figure 7. Waveform at different output voltage levels

Figure 8 illustrates the variation in the duty cycle values of the auto-tuning PID controller implemented for the DC–DC buck converter. The duty cycle (D) is calculated using the standard formula $D=V_o/V_i$, where V_o represents the output voltage and V_i denotes the input voltage. For this study, the input voltage is taken as $V_i=20$ V. The duty cycle response to the step reference of the output voltage is also presented. When the output voltage is regulated at 12 V (for $t < 0.2$ s), the corresponding duty cycle is approximately 0.6. In the interval between 0.2 s and 0.4 s, the output voltage is reduced to 10 V, and the duty cycle accordingly decreases to 0.5.

The duty cycle is dynamically adjusted to achieve the desired output voltage. This highlights the controller’s ability to maintain steady-state performance under varying operating conditions. Variations observed in the duty cycle demonstrate the efficiency of the auto-tuning mechanism for minimizing voltage regulation errors.

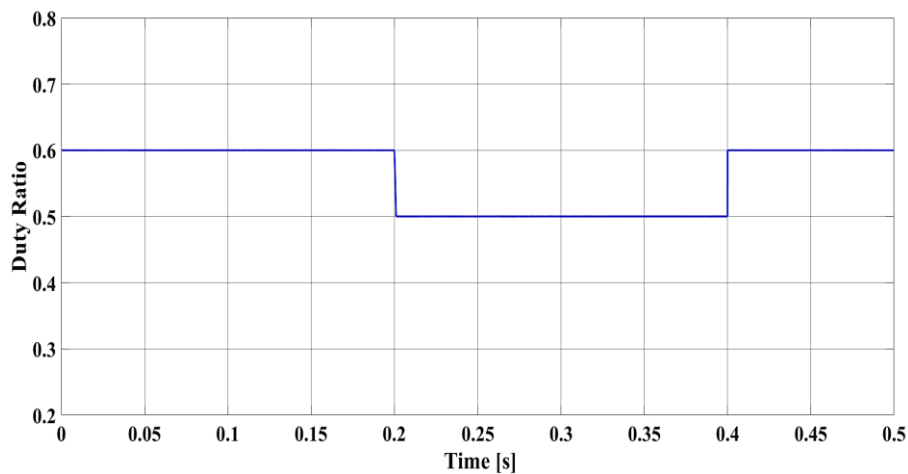


Figure 8. Duty ratio at different output voltage levels

Finally, the response of the DC–DC buck converter and the corresponding duty ratio under an exponential reference voltage change is analyzed using the auto-tuning PID controller. The converter reaches the desired reference output voltage in approximately 0.15 s, demonstrating fast transient performance. The results confirm that the proposed controller is capable of tracking the reference voltage quickly and stably. Figure 9 illustrates the output voltage waveform under exponential reference change, while Figure 10 shows the variation of the duty ratio under the same conditions. Consistently, when the reference output voltage reaches 12 V, the duty cycle converges to approximately 0.6, as determined by the relation $D=V_o/V_i$.

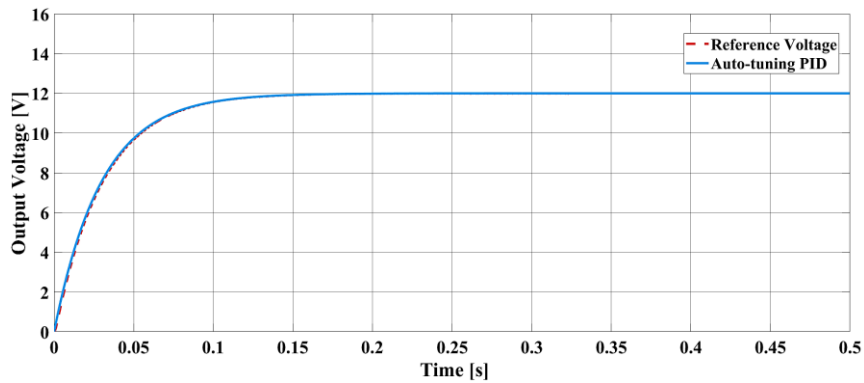


Figure 9. Waveform at exponential output voltage level

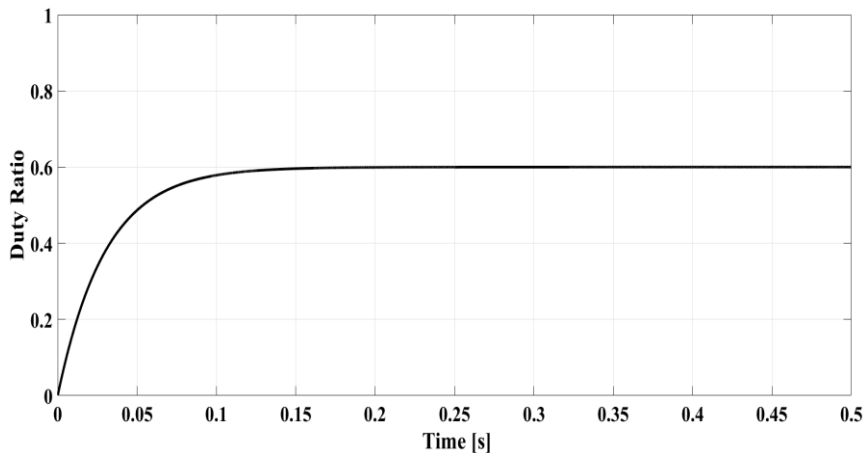


Figure 10. Duty ratio at exponential output voltage levels

The simulation results demonstrate that the proposed controller is not only responsive but also stable under different operating conditions. Fast response time and reduced overshoot emerge as key performance indicators of a well-tuned PID controller. The investigation of different load conditions further highlights the importance of adaptive control strategies in power electronics, particularly in applications that require precise voltage regulation. In this study, a comparison with the conventional PID controller was carried out by evaluating the transient responses of the DC–DC buck converter output voltages. The results reveal that the auto-tuning PID controller reaches the desired output voltage faster and without overshoot compared to the conventional PID controller.

A major advantage of the auto-tuning PID controller is its ability to automatically adjust parameters in real time, eliminating the need for manual gain tuning as in conventional PID controllers. This feature significantly reduces design effort and provides time savings. Furthermore, it adapts rapidly to changes in operating conditions, thereby minimizing overshoots, shortening rise time, and delivering a more stable transient response. Its straightforward applicability to different buck converter circuits and robustness under varying operating points further underlines the potential of the proposed method. Nevertheless, some limitations should be noted. The auto-tuning PID algorithm may require additional computational resources and memory on microcontrollers. Moreover, its performance may vary depending on circuit parameters, and uniform results across different converters cannot always be guaranteed.

The proposed controller shows strong potential for industrial applications such as renewable energy systems (solar and wind energy–based applications), battery management systems, and DC–DC converters in electric vehicles. Future work will focus on developing an experimental prototype of the DC–DC buck converter and implementing the auto-tuning PID controller in real time on high-speed platforms such as FPGAs and DSPs.

4. Conclusion

This study presented a model-based auto-tuning PID control strategy for regulating the output voltage of a DC-DC Buck converter, a widely used component in power electronics and renewable energy systems. The proposed controller was implemented in the MATLAB/Simulink environment and compared with a conventional fixed-parameter PID controller to evaluate its performance under both constant and dynamic operating conditions.

The simulation results clearly indicate that the auto-tuning PID controller significantly enhances system performance. Specifically, it achieves a faster transient response, reduced overshoot, and lower output voltage ripple when compared to conventional PID controllers. By adjusting its parameters in real time, the controller demonstrates robust adaptability to variations in system dynamics. This adaptive tuning mechanism effectively minimizes steady-state error and improves overall system stability, eliminating the need for manual retuning.

Additionally, the auto-tuning mechanism effectively shortens the time required to reach the desired reference voltage, especially during the initial transient period, while also reducing oscillations in the output voltage. These improvements are particularly valuable for precision power applications where rapid and accurate voltage regulation is essential.

In conclusion, the proposed auto-tuning PID control method offers a flexible and high-performance alternative to traditional fixed-gain PID controllers. Its ability to dynamically adapt to varying conditions makes it a promising solution for improving the efficiency and reliability of DC-DC Buck converters in real-world applications.

5. Author Contribution Statement

The author was responsible for the conceptualization and design of the study, conducting the literature review, analyzing the results obtained, acquiring and processing the data, and interpreting the findings. Additionally, the author reviewed the manuscript for both content and grammatical accuracy, ensuring its final form was ready for submission.

6. Ethics Committee Approval and Conflict of Interest Declaration

The author confirms that there are no conflicts of interest or personal relationships that could have influenced the results presented in this paper. Additionally, no external funding was received for this research. The data supporting the conclusions of this study can be provided upon request from the corresponding author. However, due to privacy and ethical considerations, the data cannot be made publicly available.

7. Ethical Statement Regarding the Use of Artificial Intelligence

No artificial intelligence-based tools or applications were used in the preparation of this study. The entire content of the study was produced by the author in accordance with scientific research methods and academic ethical principles.

8. References

- [1] A. Boutaghlaline, E. K. Khadiri, and A. Tahiri, "An op-amp-based PID control of DC-DC buck converter for automotive applications," *WSEAS Trans. Syst. Control*, vol. 18, 2023.
- [2] K. Gaouzi, H. El Fadil, A. Rachid, F. Z. Belhaj, and F. Giri, "Constrained model predictive control for DC-DC buck power converters," in *Proc. Int. Conf. Electr. Inf. Technol. (ICEIT)*, 2017, pp. 1–5.
- [3] K. Bendaoud, S. Krit, J. Laassiri, and L. E. Maimouni, "Modelling and simulation of DC-DC power converter buck for mobile applications using MATLAB/Simulink," *Int. J. Intell. Enterprise*, vol. 4, no. 1/2, pp. 76–87, 2017.
- [4] M. Gupta and S. P. Phulambrikar, "Design and analysis of buck converter," *Int. J. Eng. Res. Technol.*, vol. 3, no. 3, pp. 2346–2350, 2014.
- [5] K. Sharma and D. K. Palwalia, "Design of digital PID controller for voltage mode control of DC-DC converters," in *Proc. Int. Conf. Microelectron. Devices Circuits Syst. (ICMDCS)*, 2017, pp. 1–6.
- [6] N. B. M. Posdzi and R. B. A. Ran, "Design buck converter with variable switching frequency by using MATLAB Simulink simulation," *Int. J. Technol. Innov. Humanities*, vol. 1, no. 1, pp. 1–6, 2020.
- [7] A. A. A. Ismail and A. Elnady, "Advanced drive system for DC motor using multilevel DC/DC buck converter circuit," *IEEE Access*, vol. 7, pp. 54167–54178, 2019.
- [8] S. Kamat and S. Jadhav, "Design and simulation of low-power charging station for electric vehicles," in *Proc. Int. Conf. Adv. Comput. Commun. Control (ICAC3)*, 2019, pp. 1–4.
- [9] A. A. Patil, D. S. Chavan, and S. V. Yadav, "Output voltage control scheme for standalone wind energy system," in *Proc. Int. Conf. Comput. Power Energy Inf. Commun. (ICCPEIC)*, 2016, pp. 534–541.
- [10] K. Pal and M. Pattnaik, "Performance of a synchronous buck converter for a standalone PV system: An experimental study," in *Proc. IEEE 1st Int. Conf. Energy Syst. Inf. Process. (ICESIP)*, 2019, pp. 1–6.
- [11] H. El Fadil, F. Giri, F.-Z. Chaoui, and O. El Magueri, "Accounting for input limitation in the control of buck power converters," *IEEE Trans. Circuits Syst. I*, vol. 56, no. 6, pp. 1260–1271, 2009.
- [12] S. C. Tan, Y. M. Lai, M. K. H. Cheung, and C. K. Tse, "A pulse-width-modulation based sliding mode controller for buck converters," in *Proc. IEEE 35th Annu. Power Electron. Spec. Conf.*, vol. 5, 2004, pp. 3647–3653.
- [13] C. Vlad, P. Rodriguez-Ayerbe, E. Godoy, and P. Lefranc, "Explicit model predictive control of buck converter," in *Proc. 15th Int. Power Electron. Motion Control Conf. (EPE/PEMC)*, 2012.
- [14] S. Yan, A. R. Beig, and I. Boiko, "Auto-tuning of DC-DC buck converters through the modified relay feedback test," *IEEE Access*, vol. 9, pp. 62505–62518, 2021.
- [15] O. Saleem, K. R. Ahmad, and J. Iqbal, "Fuzzy-augmented model reference adaptive PID control law design for robust voltage regulation in DC–DC buck converters," *Mathematics*, vol. 12, p. 1893, 2024.
- [16] L. Fong, M. Islam, and M. Ahmad, "Optimized PID controller of DC-DC buck converter based on Archimedes optimization algorithm," *Int. J. Robot. Control Syst.*, vol. 3, no. 4, pp. 658–672, 2023.
- [17] H. A. Syahidah, A. J. Pangestu, M. S. Al Farisi, R. Ferdiansyah, R. N. Warnata, M. Zulfikar, and M. A. Rizqulloh, "Design and implementation of a digital PID controller for DC–DC buck converter with MATLAB," *J. Mechatronics Artif. Intell.*, vol. 2, no. 2, pp. 1–20, 2025.
- [18] S. Iplikci, "A comparative study on a novel model-based PID tuning and control mechanism for nonlinear systems," *Int. J. Robust Nonlinear Control*, vol. 20, no. 13, pp. 1483–1501, 2010.
- [19] M. Cetin and S. Iplikci, "A novel auto-tuning PID control mechanism for nonlinear systems," *ISA Trans.*, vol. 58, pp. 292–308, 2015.
- [20] M. H. Rashid, *Power Electron. Handbook*, 4th ed. Oxford, U.K.: Academic Press, 2017.
- [21] J. Pathan, "Model predictive control of DC-DC buck converter and its comparison with PID controller," *Int. J. Adv. Res. Eng. Technol.*, vol. 11, no. 9, pp. 362–367, 2020. [Online]. Available: <https://ssrn.com/abstract=3713708>

- [22] R. Sampath, "Digital peak current mode control of buck converter using MC56F8257 DSC," Appl. Note AN4716, Rev. 1, Freescale Semiconductor, 2013.
- [23] S. Satpathy, S. Ghosh, S. Das, S. Debbarma, and B. K. Bhattacharyya, "Study of dynamic response of DC-DC buck converter based on PID controller," *Int. J. Comput. Intell. IoT*, vol. 2, no. 4, 2018. [Online]. Available: <https://ssrn.com/abstract=3361548>
- [24] R. K. Sharma, "PI controller design for DC buck converter connected to a PV cell," Master's thesis, Lovely Professional University, 2015.